

Double resonance in the infinite-range quantum Ising model

Sung-Guk Han,¹ Jaegon Um,² and Beom Jun Kim^{1,*}

¹*Department of Physics and BK21 Physics Research Division,
Sungkyunkwan University, Suwon 440-746, Korea*

²*School of Physics, Korea Institute for Advanced Study, Seoul 130-722, Korea*

We study quantum resonance behavior of the infinite-range kinetic Ising model at zero temperature. Numerical integration of the time-dependent Schrödinger equation in the presence of an external magnetic field in the z direction is performed at various transverse field strengths g . It is revealed that two resonance peaks occur when the energy gap matches the external driving frequency at two distinct values of g , one below and the other above the quantum phase transition. From the similar observations already made in classical systems with phase transitions, we propose that the double resonance peaks should be a generic feature of continuous transitions, for both quantum and classical many-body systems.

PACS numbers: 75.10.Jm, 05.40.-a, 05.30.Rt

I. INTRODUCTION

A noise is often considered as a nuisance for a system to display any ordered behavior, and thus the weaker the better for the performance of the system. However, for the last decades, a lot of researchers have revealed that this is not always the case and that there exist a class of systems in which the intermediate strength of noise can help the system to show the best coherence with an external periodic driving. This surprising phenomenon was termed as the stochastic resonance (SR) due to its stochastic nature [1]. The phenomenon of SR has been found in the fields of physics and earth science, as well as in biology: the periodically recurrent ice ages, the bistable ring laser, superconducting quantum interference device, human vision and the auditory system, and the feeding mechanism of paddle fish, to list a few [1, 2]. The occurrence of the SR is properly explained by the time-scale matching condition: the coherence between the system's response and the external driving becomes strongest when the stochastic time scale inherent in the system matches the time scale provided by the external driving. In a simple classical system of a few degrees of freedom making contact with a thermal reservoir, the intrinsic time scale is given by the monotonically decreasing function of the exponential thermal activation form. Accordingly, the above mentioned time-scale matching condition can only be satisfied at a single temperature [1]. The time-scale matching condition was later extended to the classical statistical mechanical systems with continuous phase transitions such as the globally coupled, i.e., infinite-range kinetic Ising model [3]. It has been shown that the nonmonotonic behavior of the intrinsic time scale around the critical temperature makes the time-scale matching condition satisfied at two distinct temperatures, one below and the other above the critical temperature, resulting in the double resonance

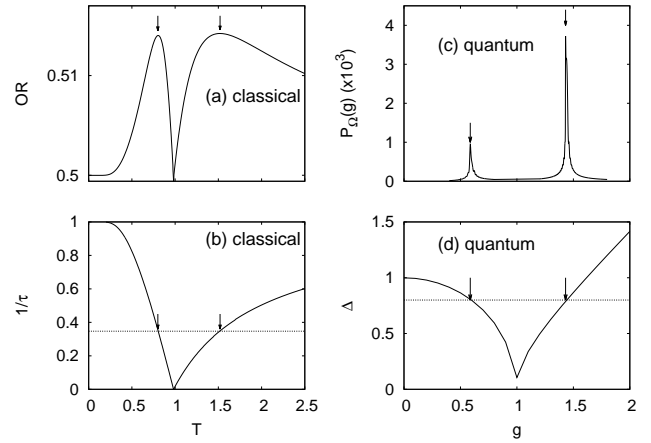


FIG. 1. Infinite-range (a)-(b) classical and (c)-(d) quantum Ising models. Double SR peaks are observed in (a) the occupancy ratio (OR, the fraction of spins in the direction of the external periodic driving), and in (c) the power spectrum at the driving frequency Ω , $P_{\Omega}(g) \equiv |\int dt e^{i\omega t} m(t;g)|_{\omega=\Omega}^2$, where $m(t;g)$ is the magnetization. Fluctuation strength is controlled by (a) the temperature T and (c) the transverse field strength g , respectively. Arrows denote the positions of maxima in (a) and (c), which are in good agreements with the time scale matching conditions shown in (b) and (d). In (b) τ is the intrinsic relaxation time scale, and in (d) Δ is the energy gap (and thus the inverse time scale). The dotted horizontal lines in (b) and (d) denote the external frequency scales of time-periodic driving. Δ in (d) is obtained from the direct diagonalization of the quantum Hamiltonian for the system size $N = 1000$ and $P_{\Omega}(g)$ in (c) through the semiclassical approximation on the Heisenberg equation of motion (see text). See [3] for (a) and (b).

peaks. The double SR peaks have also been observed in the classical Heisenberg spin system in a planar thin film geometry [4], and infinite-range q -state clock model [5].

The SR phenomenon in quantum systems, named as quantum stochastic resonance (QSR), has been studied with focus on the interplay between quantum and clas-

* Corresponding author: beomjun@skku.edu

sical fluctuation at finite temperatures [1, 6]. The QSR at zero temperature has also been studied for the one-dimensional quantum spin system with a spatially modulated external field, and the length-scale matching similar to the time-scale matching in conventional SR has been discussed [7]. In the present work, we study the QSR at zero temperature in the Ising spin system with the quantum phase transition [8]. We summarize our main findings in Fig. 1, which displays the double SR peaks and the time-scale matching conditions in infinite-range classical [3] and quantum (this work) Ising systems in the presence of a weak external driving with the frequency Ω . We conclude that the time-scale matching condition allows us to understand the classical and the quantum double SR peaks on the same ground.

In this paper, we numerically study the resonance behavior of the infinite-range quantum Ising model. Integrations of the time-dependent Schrödinger equation and the semiclassical equation of motion unanimously yield the existence of the double SR peaks, which are clearly explained from the matching condition between the energy gap, which is intrinsic, and the frequency of the external time periodic driving.

II. RESULTS

Let us begin with the globally coupled N spins described by the Hamiltonian $H = -1/(2NS) \sum_{j \neq k} S_j^z S_k^z - g \sum_j S_j^x$, where S_j^α is the spin-1/2 operator in the α direction ($\alpha = x, y, z$) at the j th site ($S \equiv 1/2$ and $\hbar \equiv 1$ henceforth), and the transverse field g in the x direction induces quantum fluctuation due to $[S_j^z, S_j^x] = i\delta_{jk} S_j^y \neq 0$. By using the total spin operator $J_\alpha \equiv \sum_j S_j^\alpha$ with $J = N/2$, the Hamiltonian can be cast into the form [9]

$$H = -\frac{1}{2J} J_z^2 - g J_x, \quad (1)$$

which allows us to handle much bigger N since the number of base kets becomes only $N + 1$ (we use J_z eigenkets as base kets). The globally coupled quantum Ising model Eq. (1) is very well-known to exhibit the quantum phase transition of the mean-field nature and its finite-size scaling has also been extensively studied [9] (see [10] for the finite-size scaling of the quantum phase transition in the one-dimensional Ising chain system).

We numerically obtain the energy gap Δ between the ground and the first-excited states of the Hamiltonian Eq. (1), which exhibits the quantum phase transition at $g = g_c = 1$ of the mean-field universality class as displayed in Fig. 2 for the system sizes $N = 200, 600$, and 1000. The inset of Fig. 2 shows the finite-size scaling of Δ with the well-known exponents: dynamic critical exponent $z = 1$, the correlation length exponent $\nu = 1/2$, and the upper critical dimension $d_c = 3$ [9]. The vanishing energy gap (and thus the divergence of the intrinsic time scale) at the quantum critical point is particularly

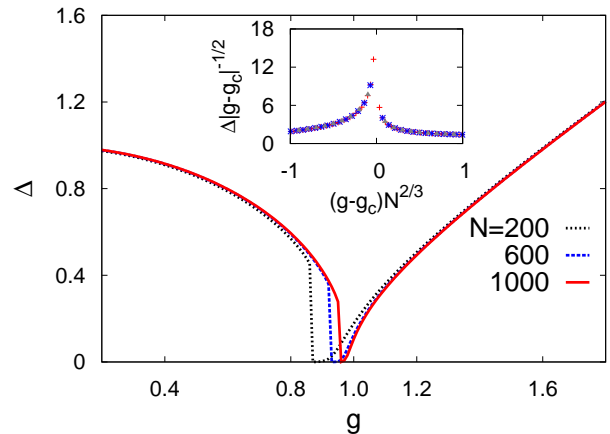


FIG. 2. (Color online) The energy gap Δ between the ground and the first-excited states versus the transverse field strength g for the globally-coupled quantum Ising model without external driving in z -direction. Δ vanishes as the quantum critical point $g_c = 1$ is approached. Inset: Finite-size scaling of the form $\Delta = (g - g_c)^{z\nu} f[(g - g_c)N^{1/d_c\nu}]$ with $z = 1$, $\nu = 1/2$, and $d_c = 3$.

important in the present study: The nonmonotonicity of Δ as a function of the fluctuation strength g provides the origin of the double quantum resonance peaks (see Fig. 1).

In parallel to studies of the classical SR behaviors [1, 3], we next apply the weak time-periodic external magnetic field $h(t) = h_0 \cos \Omega t$ along the z -direction with $h_0 = 10^{-3}$ and $\Omega = 0.8$, to get the time-dependent Schrödinger equation

$$i \frac{d|\Psi(t)\rangle}{dt} = \left[-\frac{1}{N} J_z^2 - g J_x - h(t) J_z \right] |\Psi(t)\rangle, \quad (2)$$

where the quantum ket $|\Psi(t)\rangle = \sum_{M=-J}^J A_M(t) |M\rangle$ with $J_z |M\rangle = M |M\rangle$ and the complex coefficient $A_M(t)$. The time evolution of the system is numerically traced through the use of the fifth-order Runge-Kutta method combined with the Richardson extrapolation and Bulirsch-Stoer method [11]. We check that the use of the sufficiently small time step $\delta t = 10^{-4}$ keeps the normalization condition $\sum |A_M(t)|^2 = 1$ unchanged within numerical accuracy. We first get the ground state in the presence of the extremely small external field in the positive z -direction to break the up-down spin symmetry, and use it as the initial condition for Eq. (2).

As the most important quantity to detect SR behavior, the average magnetization in the z direction $m(t) \equiv (1/J) \langle \Psi(t) | J_z | \Psi(t) \rangle$ is measured as a function of time. We do not observe significant difference for other system sizes, and we display our results $m(t)$ for $N = 600$ in Fig. 3 at (a) below and (b) above the quantum critical point $g_c = 1$. When $g > g_c$, $m(t)$ oscillates around $m = 0$, and we shift vertically each $m(t)$ in Fig. 3(b) for better comparison. It is obvious from Fig. 3 that the resonance behavior of $m(t)$ is seen in the form of

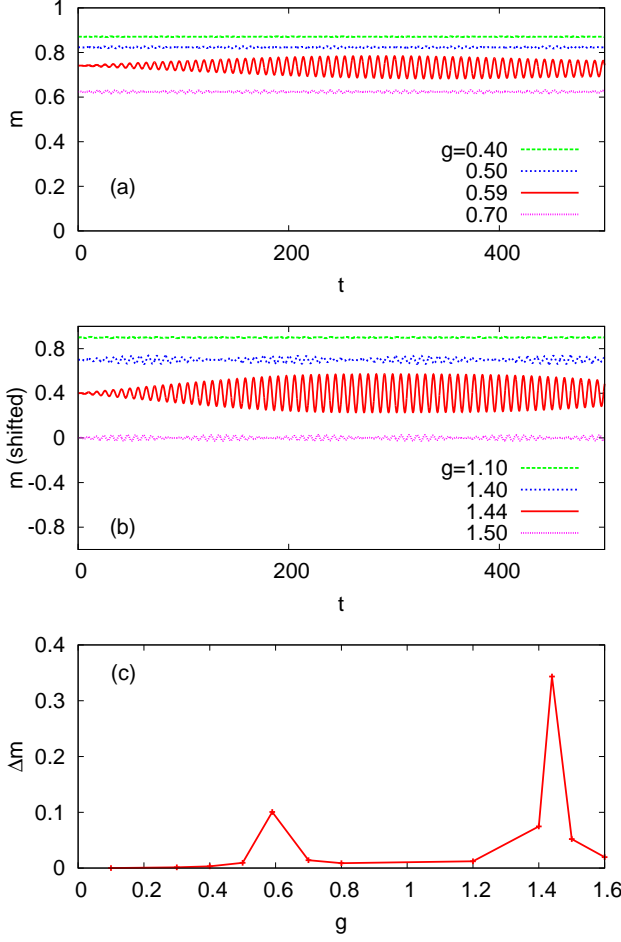


FIG. 3. (Color online) The order parameter $m(t) = (1/N) \langle \Psi(t) | J_z | \Psi(t) \rangle$ in time t at (a) $g < g_c = 1$ and (b) $g > g_c$ for $N=600$ in the presence of an external oscillating magnetic field $h_0 \cos \Omega t$ with $\Omega=0.8$ in the z direction. At two values of g , one at $g_1 \simeq 0.59$ and the other at $g_2 \simeq 1.44$, $m(t)$ exhibits the larger oscillation amplitude reflecting the stronger coherence with the external driving. For better distinction, $m(t)$ is vertically shifted by 0.9, 0.7, 0.4, and 0 at $g = 1.10, 1.40, 1.44$, and 1.50 in (b), respectively. (c) The oscillation amplitude Δm versus g , exhibiting double SR peaks.

the larger oscillation amplitude at *two* distinct strengths of quantum fluctuation, i.e., one below g_c and the other above g_c . In Fig. 3(c), we display the oscillation amplitude $\Delta m \equiv \max_t m(t) - \min_t m(t)$, which clearly shows double resonance peaks. We denote the first and the second resonance points as $g_1 \approx 0.59$ and $g_2 \approx 1.44$, where the oscillation amplitudes become maxima. As another indicator of the SR behavior, we carry out the Fourier transformation of $m(t)$ to obtain $m(\omega)$ at frequency ω . Figure 4 displays the magnitude of the spectral components $|m(\omega)|$ versus ω at various values of g . In general, there exist two peaks in $|m(\omega)|$, one at $\omega_1 = \Omega = 0.8$ [indicated by the dotted vertical lines in Fig. 4], and the other at the position ω_2 that depends on g . We observe that the latter peak at ω_2 simply originates from the en-

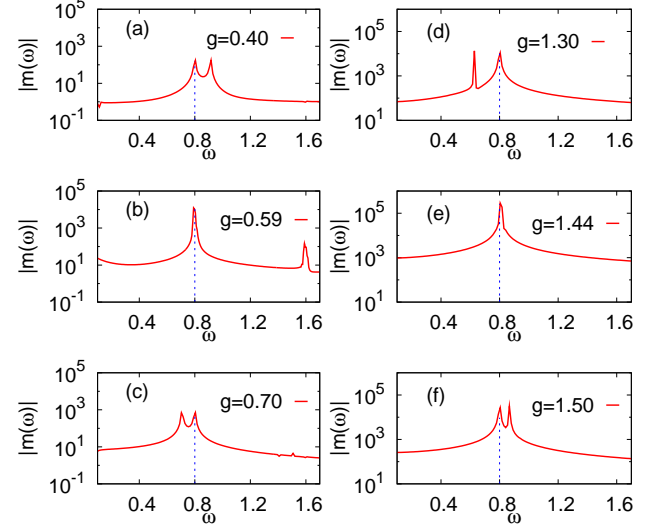


FIG. 4. (Color online) The magnitude of the power spectral density $|m(\omega)|$ versus frequency ω at various values of the transverse field strength g . The dashed vertical lines denote the frequency of the external field ($\Omega = 0.8$). At $g = 0.59$ and 1.44 , the two peaks in the spectral density merge to become one. The peak in (b) at $\omega=1.6$ is a harmonics, and does not reflect the energy gap like peaks in other panels.

ergy gap (see Fig. 2), i.e., $\omega_2 = \Delta$ (note that $\hbar = 1$ in this work). As g is increased toward g_c from below, Δ decreases (see Fig. 2), which in turn yields decreasing ω_2 as shown in Fig. 4(a)-(c). As g passes through g_c from below, ω_2 bounces back and moves to a larger value, reflecting the increase of Δ for $g > g_c$ in Fig. 2. Another important observation one can make from Fig. 4 is that when the two peaks at ω_1 and ω_2 merge into a single one at $\omega = \omega_1 = \Omega$, the power spectrum ($P_\omega = |m(\omega)|^2$) at Ω suddenly increases much. From this, it is clear that the merging of the two peaks must occur at two distinct values of g , which are in good agreement with $g_1 \approx 0.59$ and $g_2 \approx 1.44$ in Fig. 3.

We next adopt the Heisenberg picture in which the spin operator satisfies the equation of motion $\dot{J}_\alpha = -i[H, J_\alpha]$. By using the commutation relation $[J_\alpha, J_\beta] = i\epsilon_{\alpha\beta\gamma}J_\gamma$, we get $\dot{J}_x = (1/2J)(J_z J_y + J_y J_z) + h(t)J_y$, $\dot{J}_y = -(1/2J)(J_z J_x + J_x J_z) + gJ_z - h(t)J_x$, and $\dot{J}_z = -gJ_y$. We then make the semiclassical approximation and treat the spin operator J_α as the α -th component of the classical spin vector $\vec{J} \equiv J(\sin \theta \cos \phi, \sin \theta \sin \phi, \cos \theta)$, which results in [9, 12]

$$\begin{aligned} \dot{\theta} &= g \sin \phi, \\ \dot{\phi} &= g \cot \theta \cos \phi - \cos \theta - h(t). \end{aligned} \quad (3)$$

We take initial values of θ and ϕ from the ground state of the system calculated by semiclassical approximation of Eq. (1), and perform numerical integrations of Eq. (3) in time at given values of g . In this semiclassical ap-

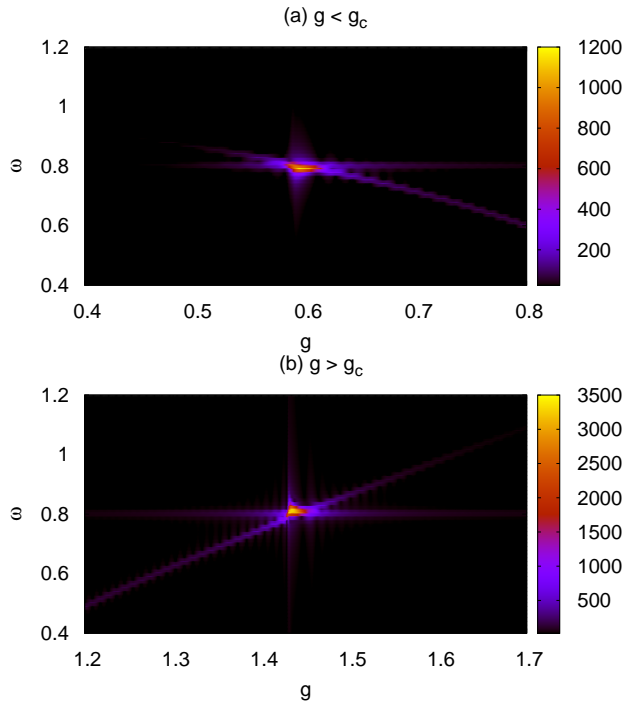


FIG. 5. (Color online) $|m(\omega)|$ versus g and ω in the two regions (a) $g < g_c = 1$ and (b) $g > g_c = 1$ obtained via semiclassical approximation applied for the Heisenberg equations of motion. The right panels of (a) and (b) show the color scheme for $|m(\omega)|$. Along $\omega = 0.8$ axis, as g is increased, $|m(\omega)|$ exhibits the biggest value both at $g \simeq 0.59$ and $g \simeq 1.44$.

proximation, the order parameter is simply computed from $m(t) = J_z/J = \cos\theta(t)$, which is then used for the Fourier analysis. We again find the SR behaviors at

two distinct values of g : $g_1 \simeq 0.59$ and $g_2 \simeq 1.44$ as displayed in Fig. 5, which are in perfect agreement with the findings in Fig. 4.

III. SUMMARY

In summary, the infinite-range quantum transverse-field Ising model at zero temperature has been numerically investigated in the presence of the weak longitudinal time-periodic magnetic field at the frequency Ω . The resonance behavior at two distinct values of the transverse field g has been clearly observed via (i) the large amplitude oscillation of the magnetization in time and (ii) the large peak at Ω in spectral analysis. The origin of the double SR peaks in the system has been identified from the vanishing of the energy gap around the quantum critical point. When the energy gap matches the frequency of the external field, the strong resonance peaks occur at two different values of g , exhibiting the double resonance behavior. We have also confirmed the double resonance in the thermodynamic limit through the use of the semiclassical approximation made for the Heisenberg equation of motion. We propose that the time-scale matching condition should play an important role in understanding the double SR behavior in a broad range of systems with continuous phase transitions, both classical and quantum.

ACKNOWLEDGEMENTS

This work was supported by the National Research Foundation of Korea (NRF) grant funded by the Korea government (MEST) via No. 2011-0015731.

-
- [1] L. Gammaritoni, P. Hänggi, P. Jun, and F. Marchesoni, *Rev. Mod. Phys.* **70**, 223 (1998).
 - [2] R. Benzi, G. Parisi, A. Sutera, and A. Vulpiani, *Tellus* **34**, 10 (1982); B. McNamara, K. Wiesenfeld, and R. Roy, *Phys. Rev. Lett.* **60**, 2626 (1988); A. D. Hibbs, A. L. Singaas, E. W. Jacobs, A. R. Bulsara, J. J. Bekkedahl, and F. Moss, *J. Appl. Phys.* **77**, 2582 (1995); R. Rouse, S. Han, and J. E. Lukens, *Appl. Phys. Lett.* **66**, 108 (1995); E. Simonotto, M. Riani, C. Seife, M. Roberts, J. Twitty, and F. Moss, *Phys. Rev. Lett.* **78**, 1186 (1997); F. Jaramillo and K. Wiesenfeld, *Nat. Neurosci.* **1**, 384 (1998); D.F. Russell, L.A. Wilkens, and F. Moss, *Nature* **402**, 291 (1999).
 - [3] B. J. Kim, P. Minnhagen, H. J. Kim, M. Y. Choi, and G. S. Jeon, *Europhys. Lett.* **56**, 333 (2001).
 - [4] H. Jang, M. J. Grimson, and C. K. Hall, *Phys. Rev. B* **67**, 094411 (2003).
 - [5] S. K. Baek and B. J. Kim **86**, 011132 (2012).
 - [6] R. Löfstedt and S. N. Coppersmith, *Phys. Rev. Lett.* **72**, 1947 (1994); M. Grifoni and P. Hänggi, *ibid.* **76**, 1611 (1996); M. Grifoni, L. Hartmann, S. Berchtold, and P. Hänggi, *Phys. Rev. E* **53**, 5890 (1996); K. Dong and N. Makri, *Phys. Rev. A* **70**, 042101 (2004); S. F. Huelga and M. B. Plenio, *Phys. Rev. Lett.* **98**, 170601 (2007).
 - [7] P. Sen, *Phys. Rev. E* **63**, 040101(R) (2001).
 - [8] See, e.g., S. Sachdev, *Quantum Phase Transition* (Cambridge University Press, Cambridge, 1999) for quantum phase transition in spin systems.
 - [9] R. Botet and R. Jullien, *Phys. Rev. B* **28**, 3955 (1983).
 - [10] J. Um, S.-I. Lee, and B. J. Kim, *J. Kor. Phys. Soc.* **50**, 285 (2007).
 - [11] W. H. Press, S. A. Teukolsky, W. T. Vetterling, and B. P. Flannery, *Numerical Recipes in C* (2nd Ed., Cambridge University Press, Cambridge, 1992).
 - [12] A. Das, K. Sengupta, D. Sen, and B. K. Chakrabarti, *Phys. Rev. B* **74**, 144423 (2006).